This article has not been copyedited and formatted. The final version may differ from this version.
DMD Fast Forward. Published on December 13, 2010 as doi: 10.1124/dmd.110.035998

Measurement of Unbound Drug Exposure in Brain: Modelling of pH Partitioning Explains Diverging Results between the Brain Slice and Brain Homogenate Methods

Markus Fridén, Fredrik Bergström, Hong Wan, Mikael Rehngren, Gustav Ahlin, Margareta Hammarlund-Udenaes and Ulf Bredberg.

Division of Pharmacokinetics and Drug Therapy, Department of Pharmaceutical Biosciences, Uppsala University, Sweden (M.F., M. H-U)

Discovery DMPK, AstraZeneca R&D, Mölndal, Sweden (M.F., M.R., U.B.)

Lead Generation, AstraZeneca R&D, Mölndal, Sweden (F.B., H.W.)

Pharmaceutical Screening and Informatics, Department of Pharmacy, Uppsala University (G.A.)

DMD Fast Forward. Published on December 13, 2010 as DOI: 10.1124/dmd.110.035998
This article has not been copyedited and formatted. The final version may differ from this version.

A. Running title:

Comparison of the brain slice and brain homogenate methods

B. Corresponding author:

Markus Fridén

Division of Pharmacokinetics and Drug Therapy

Department of Pharmaceutical Biosciences

Uppsala University

Box 591

SE-751 24 Uppsala

Sweden

Tel +46 – (0) 31 706 5360

Fax +46 – (0) 31 776 37 86

E-mail: Markus.Friden@farmbio.uu.se

C.

Number of text pages:	38	
Number of tables:	1	
Number of figures:	8	
Number of references:	35	
Number of words in	Abstract:	250 (Max 250)
	Introduction:	705 (Max 750)
	Discussion:	1518 (Max 1500)

D, Non standard abbreviations:

DMD Fast Forward. Published on December 13, 2010 as DOI: 10.1124/dmd.110.035998
This article has not been copyedited and formatted. The final version may differ from this version.

ABC - ATP-binding cassette

BCRP - breast cancer resistance-associated protein

CNS - central nervous system

CIR - confidence Interval Ratio

$C_{u,brainISF}$ - unbound drug concentration in brain interstitial fluid

$f_{u,brain}$ - fraction of unbound drug in the brain

ISF - interstitial fluid

$K_{p,uu,cell}$ - unbound partition coefficient of the cell

LC-MS/MS - liquid chromatography tandem mass spectrometry

MRP - multidrug resistance protein

MPP - 1-methyl-4-phenylpyridinium

OCT - organic cation transporter

TEA - tetraethylammonium

$V_{u,brain}$ - unbound volume of distribution in brain

DMD Fast Forward. Published on December 13, 2010 as DOI: 10.1124/dmd.110.035998
This article has not been copyedited and formatted. The final version may differ from this version.

Abstract

Currently used methodology for determining unbound drug exposure in brain combines measurement of the total drug concentration in the whole brain in vivo with estimation of brain tissue binding from one of two available in vitro methods: equilibrium dialysis of brain homogenate and the brain slice uptake method. This study of 56 compounds compares the fraction of unbound drug in brain ($f_{u,brain}$), determined using the brain homogenate method, with the unbound volume of distribution in brain ($V_{u,brain}$), determined using the brain slice method. Discrepancies were frequent and primarily related to drug pH partitioning, due to the preservation of cellular structures in the slice that are absent in the homogenate. A mathematical model for pH partitioning into acidic intracellular compartments was derived to predict the slice $V_{u,brain}$ from measurements of $f_{u,brain}$ and drug pKa. This model allowed prediction of $V_{u,brain}$ from $f_{u,brain}$ within a 2.2-fold error range for 95% of the drugs, as compared to a 4.5-fold error range using the brain homogenate $f_{u,brain}$ method alone. The greatest discrepancies between the methods occurred with compounds that are actively transported into brain cells, including gabapentin, metformin and prototypic organic cation transporter substrates. It is concluded that intra-brain drug distribution is governed by several diverse mechanisms in addition to non-specific binding and that the slice method is therefore more reliable than the homogenate method. Alternatively, predictions of $V_{u,brain}$ can be made from homogenate $f_{u,brain}$ using the presented pH partition model, although this model does not take into consideration possible active brain cell uptake.

DMD Fast Forward. Published on December 13, 2010 as DOI: 10.1124/dmd.110.035998
This article has not been copyedited and formatted. The final version may differ from this version.

Introduction

Measurement of exposure of the brain to drugs is frequently undertaken in the drug discovery process to evaluate the influence of the blood-brain barrier (BBB) on the uptake of drugs and to evaluate central drug effects. The drug molecules that are not bound to brain tissue are the pharmacologically active entities, and the concentration of unbound drug in the brain interstitial fluid ($C_{u,brainISF}$) is the most important parameter for estimating brain exposure; the ratio of $C_{u,brainISF}$ to plasma unbound drug concentrations is particularly useful. The brain-to-plasma ratio of unbound drug concentrations, known as $K_{p,uu,brain}$ or $K_{p,free}$, provides an explicit value for the extent of BBB transport, i.e. brain exposure normalized to systemic exposure. Until recently, microdialysis has been the only method of measuring $C_{u,brainISF}$ and $K_{p,uu,brain}$, but the associated technical challenges have precluded broad implementation of this method in the drug discovery process. In some instances drug concentrations in cerebrospinal fluid have been measured as alternative but the validity of such measurements has been questioned. Instead, methods based on whole brain concentrations have been used routinely, shaping much of the current information on the relationship between chemical structure and brain exposure, and resulting in questionable predictions of drug effects. The brain slice (Kakee et al., 1996) and brain homogenate (Mano et al., 2002, Kalvass and Maurer, 2002) methods have recently been validated for measurement of the distribution or binding of drug within brain tissue (Friden et al., 2007, Friden et al., 2009a, Liu et al., 2009). $C_{u,brainISF}$ can be calculated by combining either in vitro method with conventionally measured total drug concentrations in whole brain in vivo. The implementation of these more high-throughput methodologies has now opened the possibility of guiding the design of drugs based on data relevant to brain exposure.

The brain slice method estimates the unbound volume of distribution in brain ($V_{u,brain}$, mL*g brain^{-1}) which quantifies the overall cellular uptake of drug; the value for $V_{u,brain}$ will increase with increases in the uptake and/or binding of the drug. The brain homogenate method,

DMD Fast Forward. Published on December 13, 2010 as DOI: 10.1124/dmd.110.035998
This article has not been copyedited and formatted. The final version may differ from this version.

on the other hand, takes only non-specific binding into account and is used to determine the fraction of unbound drug in a sample of homogenized tissue ($f_{u,brain}$). Although $V_{u,brain}$ and $f_{u,brain}$ are inversely related and can be used for the same purpose, the brain homogenate method is by far the more commonly used method in the drug industry. This is probably because of the ease of setting up the assay and conducting the experiment. While the slice method can also be employed in high-throughput processes (Friden et al., 2009a),it is associated with higher initial costs and effort.

Although non-specific binding is expected to dominate intra-brain distribution, other processes are also involved. For example, one important process involves the partitioning of weak acids and bases along the pH gradient across cell membranes, which occurs because non-charged species are more likely to passively diffuse through membranes. This leads to an accumulation of basic drugs in cells because the intracellular pH is lower than the extracellular pH. Perhaps more importantly, basic drugs can be trapped in intracellular sub-compartments such as lysosomes, which can have a pH as low as 5 (Daniel et al., 1995, de Duve et al., 1974). Another important process involves the carrier-mediated transport of drugs across membranes. While the role of drug transporters at the BBB is firmly established, there is as yet little known about the impact of uptake and efflux transporters on the intra-brain distribution of drugs. Cellular uptake of, for example, gabapentin (Su et al., 1995) and 1-methyl-4-phenylpyridinium (MPP) (Gorboulev et al., 1997, Grundemann et al., 1998) is mediated by members of the solute carrier family of transporters. Further, efflux transporters belonging to the ABC super-family such as p-glycoprotein (Pgp), breast cancer resistance-associated protein (BCRP) and multidrug resistance protein 1 (MRP1) are expressed in brain parenchyma and may limit the cellular uptake of drugs (Bleasby et al., 2006, Dallas et al., 2006). All in all, drug distribution within brain tissue is far more complex than non-specific binding.

The present study was undertaken to systematically investigate the quantitative

DMD Fast Forward. Published on December 13, 2010 as DOI: 10.1124/dmd.110.035998
This article has not been copyedited and formatted. The final version may differ from this version.

relationship between $f_{u,brain}$ and $V_{u,brain}$ obtained using the two methods, and to explain the differences between the methods in terms of drug pKa values, cellular pH gradients and carrier-mediated transport.

Materials and methods

Compound selection

The 56-compound set used in this study was an extension of a previously used set of 43 physico-chemically diverse drugs belonging to five different therapeutic areas (Friden et al., 2009b). The additional 13 compounds were included mainly to address carrier-mediated transport. The added compounds were basic and cationic compounds associated with carrier-mediated cation transport; they included MPP, tetraethylammonium (TEA), neostigmine, metformin, amantadine, clonidine, three additional substrates of Pgp (N-methylquinidine, quinidine and quinine), two acidic molecules (diclofenac and fluorescein) and two neutral drugs (alprazolam and midazolam).

Chemicals

2-Ethyl-2-phenylmalonamide was purchased from Acros Organics (Geel, Belgium), amitriptyline and thioridazine were purchased from ICN Biomedicals (Eschwege, Germany), and delavirdine and gabapentin were purchased from Toronto Research Chemicals Inc. (Toronto, Canada). Morphine, morphine-3-glucoronide, morphine-6-glucuronide, oxycodone and oxymorphone were obtained from Lipomed (Arlesheim,Switzerland). Salicylic acid and tramadol were obtained from Fluka BioChemika (Poole, U.K.), moxalactam and oxprenolol were purchased from MP Biomedicals Inc. (Illkirsch, France), nelfinavir mesylate was purchased from Apin Chemicals (Abingdon, U.K.), and ^{14}C-dimethyloxazolidinedione was

purchased from American Radiolabeled Chemicals (St. Louis, MO). All other drugs and compounds were purchased from Sigma (St. Louis, MO).

Animals

Male Sprague-Dawley rats (Harlan, Horst, the Netherlands), weighing 300-400 grams, were used for the in vitro brain slice experiments and preparation of the brain homogenate. All animals were housed in groups at 18-22°C under a 12 h light-dark cycle with free access to food and water for at least five days before the experiment. The study was approved by the Animal Ethics Committee of Gothenburg (221-2008).

Protocol for brain slice experiments

$V_{u,brain}$ for the 56 compounds was determined in fresh brain slices using a previously published protocol without modifications (Friden et al., 2009a). In brief, freshly prepared 300 μm brain slices from drug-naive rats were incubated for 5 h in a buffer containing up to 10 drugs at very low concentrations (100 nM). Propranolol was included as quality control in each incubation. The unbound drug concentration in the slice interstitial fluid was taken to be equal to the drug concentration in the buffer. $V_{u,brain}$ (mL*g brain^{-1}), defined by Eq. 1, was calculated as the ratio of the amount of drug in the brain (slice) (A_{brain}, nmol*g brain^{-1}) to the measured final buffer concentration (C_{buffer}, μmol/L):

$$V_{u,brain} = \frac{A_{brain}}{C_{u,brainISF}} = \frac{A_{brain}}{C_{buffer}} \quad (1)$$

Protocol for brain homogenate experiments

Equilibrium dialysis of brain homogenate was performed as previously described (Wan et al., 2007) to determine $f_{u,brain}$ for the 56 compounds. The brain homogenate was prepared in 3

DMD Fast Forward. Published on December 13, 2010 as DOI: 10.1124/dmd.110.035998
This article has not been copyedited and formatted. The final version may differ from this version.

volumes of 180 mM phosphate buffer (pH 7.4) using the same part of the brain as that used for preparing brain slices. Equilibrium dialysis of 0.80 ml of homogenate and buffer was performed in at least triplicate for 16 h at 37°C in 1-ml Plexiglas cells mounted with a 5-kDa cutoff Diachema cellulose membrane (Dianorm GmbH, München, Germany). Compounds were pooled at concentrations of 5 µM with propranolol as quality control. An aliquot of homogenate was sampled before and after co-incubation to assess the compound stability. The average fraction of unbound drug in diluted brain homogenate ($f_{u,hD}$), i.e. the buffer-to-homogenate concentration ratio, was calculated for the replicates (Eq. 2).

$$f_{u,hD} = \frac{C_{buffer}}{C_{\text{hom}\,ogenate}} \quad (2)$$

Next, $f_{u,hD}$ was scaled to undiluted brain homogenate ($f_{u,brain}$) using:

$$f_{u,brain} = \frac{1}{1 + D\left(\frac{1}{f_{u,hD}} - 1\right)} \quad (3)$$

where *D* represents the dilution factor associated with preparation of the homogenate.

Brain slice experiments to determine distribution mechanisms

The contribution of lysosomal trapping to the $V_{u,brain}$ of a prototypic weak base (propranolol) and a prototypic weak acid (indomethacin) was studied by incubation with various concentrations of monensin, which is an antibiotic protonophore known to raise the lysosomal pH by facilitating the movement protons across membranes (Lake et al., 1987, Siebert et al., 2004). The extracellular pH, taken as the buffer pH, was measured using a pH electrode at the end of the incubation. The overall intracellular pH (pH_{cyto}) was measured in each slice using the ^{14}C-dimethyloxazolidinedione method (Waddell and Butler, 1959). The same experiment was also conducted for metformin and the permanently cationic compounds , MPP, neostigmine, N-methyl quinidine and TEA. The contribution of carrier-mediated transport of the same

cationic drugs was assessed using decynium-22 (D22), which is a known inhibitor of organic cation transporters (OCT). Propranolol was used as control. Various concentrations of D22 was tested in order ensure that results were obtained from non-toxic conditions. The effect of drug efflux by Pgp on $V_{u,brain}$ was assessed for the Pgp substrates loperamide, saquinavir, nelfinavir and N-methylquinidine using 10 µM cyclosporine A (Wang et al., 2008). Fumitremorgin C (20 µM) and MK-571 (10 µM) were used to investigate the roles of BCRP and isoforms of MRP, respectively, for the BCRP substrate mitoxantrone and the dual BCRP/MRP substrate sulphasalazine. Prior experience with using high inhibitor concentrations of e.g. verapamil (100 µM) to inhibit Pgp resulted in considerable swelling of the slices (unpublished observations). The experiments to investigate drug efflux in this study were therefore conducted using more potent inhibitors and also shorter incubation times (3 hours) in order to limit unspecific effects of the inhibitors.

pKa measurements and ion classification

Data on pKa were obtained using a novel high-throughput assay based on capillary electrophoresis coupled to mass spectrometry (CE/MS) (Wan et al., 2003, Wan and Ulander, 2006). In brief, the effective mobility of the compound was measured in a set of buffered pH solutions by CE/MS and the pKa was obtained by non-linear fit of the effective mobility as a function of pH using automated data analysis. Reference compounds were employed as on-line quality controls, which provided an accurate pKa screening within 0.2 pKa units in most cases. Compounds were classified as acids, bases, zwitterions, neutrals or permanent cations based on the predominant ionization state at pH 7.4. Hence, acids carry a net negative charge, bases carry a net positive charge (permanent cations disregarded), neutrals may or may not have acidic or basic functions but are predominantly neutral at pH 7.4, and zwitterions carry at least one acidic and one basic function which are ionized at pH 7.4.

DMD Fast Forward. Published on December 13, 2010 as DOI: 10.1124/dmd.110.035998
This article has not been copyedited and formatted. The final version may differ from this version.

Analytical procedures

The drugs were quantified by reversed-phase liquid chromatography and multiple-reaction monitoring (MRM) mass spectrometry (liquid chromatography-tandem mass spectrometry, LC-MS/MS) detection using Micromass (Waters, Sollentuna, Sweden) triple-quadrupole instruments equipped with electrospray. Alternatively, a Waters MicroMass LCT Premier TOF mass spectrometer (run with ESI and W-mode with extended dynamic range) was used for detection with the software Masslynx 4.0 and Quanlynx 4.0 for data acquisition and quantification, respectively. Gradient elution over 2-5 minutes with acetonitrile and 0.2% formic acid was used with various C18 columns. Sample preparation was adapted for any compound-specific requirements but followed a general procedure: samples of buffer and brain homogenate were added in aliquots of 50 µl to 96-deepwell plates (Nalgene Nunc International, Rochester, NY). Protein was precipitated by addition of 150 µl of cold acetonitrile containing 0.2% formic acid. After 1 min of vortexing and 20 min of centrifugation at 4000 rpm (Rotanta/TR; Hettich, Tuttlingen, Germany) at 4°C, the supernatant was transferred to a new plate and appropriately diluted with 0.2% formic acid. Samples of 5 to 20 µl from this plate were injected into the LC-MS system.

Since absolute quantification of drug is not required in the homogenate (Wan et al., 2007) or slice (Friden et al., 2009a) methods, chromatographic peak areas were used directly to calculate $f_{u,brain}$ and $V_{u,brain}$, respectively. To ensure that the responses used in the calculations were within the linear response range of the mass spectrometer, protein-precipitated samples were also diluted (10- and 100-fold) in 37.5% acetonitrile in 0.2% formic acid. These dilutions were analyzed with the un-diluted samples. Any effects of nonlinearity in response were minimized by choosing an appropriate dilution (1-, 10-, or 100-fold) such that the peak areas for, for example, buffer and homogenate were of similar size for each compound. Before

DMD Fast Forward. Published on December 13, 2010 as DOI: 10.1124/dmd.110.035998
This article has not been copyedited and formatted. The final version may differ from this version.

performing the calculations, the peak areas were scaled back to undiluted buffer and homogenate by multiplying by the dilution factors 1, 10, and 100 as appropriate.

Radioactive ^{14}C-dimethyloxazolidinedione was quantified using a Wallac WinSpectral 1414 liquid scintillation counter (Wallac, Turku, Finland) and an OptiPhase HiSafe 3 scintillation cocktail (Fisher Chemicals, Loughborough, UK). Homogenates of brain slices were solubilized with 1 ml of Soluene-350 (PerkinElmer Life and Analytical Sciences, Boston, MA) and decolourized with 100 µl of hydrogen peroxide.

Construction of pH partition models

Models were derived to describe drug distribution in brain tissue compartments by pH partitioning. The primary aim was to obtain a predictive model for the unbound drug partitioning coefficient of the cell ($K_{p,uu,cell}$), which describes the intra-to-extracellular unbound drug concentration ratio where the intracellular unbound drug concentration ($C_{u,cell}$) is the average concentration of unbound drug in various intracellular compartments (Eq. 4) (Friden et al., 2007).

$$K_{p,uu,cell} = \frac{C_{u,cell}}{C_{u,brainISF}} = f_{u,brain} \times V_{u,brain} \qquad (4)$$

If $C_{u,cell}$ is equal to $C_{u,brainISF}$, then $K_{p,uu,cell}$ = 1. For such cases, binding in tissue is the only distribution mechanism and it can be expected that $f_{u,brain}$ is equal to $1/V_{u,brain}$. However, because of pH partitioning or active transport, $C_{u,cell}$ can be greater or smaller than $C_{u,brainISF}$, resulting in values for $K_{p,uu,cell}$ that differ from unity. Accordingly, $K_{p,uu,cell}$ not only describes intracellular exposure to unbound drug but also has a potential use as a conversion factor between the brain homogenate $f_{u,brain}$ and brain slice $V_{u,brain}$ methods (Eq. 4).

The models were derived from the theory of pH partitioning (Shore et al., 1957), which assumes that membrane permeation is dominated by the non-ionized species of the drug. The

DMD Fast Forward. Published on December 13, 2010 as DOI: 10.1124/dmd.110.035998
This article has not been copyedited and formatted. The final version may differ from this version.

non-ionized fraction of the drug is pH-dependent and can be predicted from the drug pKa(s) using the Henderson-Hasselbalch equation. The concentration of non-ionized drug is equal on both sides of a biological membrane at equilibrium. However, the gross drug concentration, including that of the ionized species, can differ widely according to the pH on each side.

The tissue compartments considered were the extracellular ISF, the cytosol of the intracellular space and the acidic intracellular sub-compartments, collectively denoted lysosomes (Fig. 1). Since it was not possible to obtain information on differential non-specific binding in the various tissue compartments, it was necessary to assume a similar level of binding in all compartments.

The pH partition model for $K_{p,uu,cell}$ was constructed from its definition (Eq. 4) by combining Eq. 4 with the expression for $V_{u,brain}$ (Eq. 1):

$$K_{p,uu,cell} = f_{u,brain} \times \frac{A_{brain}}{C_{u,brainISF}} \quad (5)$$

A_{brain} is the sum of the amounts (A) of drug in each compartment, calculated as the physiological volume (V, mL*g brain^{-1}) multiplied by the concentrations of unbound drug (C_u, µM) divided by $f_{u,brain}$ in each sub-compartment, with subscripts brainISF, cyto, and lyso for brain ISF, the cell cytosol and the lysosomes, respectively (Eq. 6). The tissue density was assumed to be 1 g/mL.

$$A_{brain} = A_{ISF} + A_{cyto} + A_{lyso} = \frac{V_{ISF} \times C_{u,brainISF} + V_{cyto} \times C_{u,cyto} + V_{lyso} \times C_{u,lyso}}{f_{u,brain}} \quad (6)$$

Combining Eqs. 5 and 6 results in a 3-compartment pH partition model (Eq. 7, Fig. 1) in which $f_{u,brain}$ is cancelled:

$$K_{p,uu,cell} = V_{ISF} + K_{p,cyto} \times \left(V_{cyto} + V_{lyso} \times K_{p,lyso}\right) \quad (7)$$

where

$$K_{p,uu,cyto} = \frac{C_{u,cyto}}{C_{u,brainISF}} \quad (8)$$

DMD Fast Forward. Published on December 13, 2010 as DOI: 10.1124/dmd.110.035998
This article has not been copyedited and formatted. The final version may differ from this version.

and

$$K_{p,uu,lyso} = \frac{C_{u,lyso}}{C_{u,cyto}} \quad (9)$$

Alternatively, a simpler 2-compartment pH model was obtained by ignoring lysosome partitioning:

$$K_{p,uu,cell} = V_{ISF} + K_{p,uu,cyto} \times V_{cyto} \quad (10)$$

$K_{p,uu,cyto}$ and $K_{p,uu,lyso}$ for weak acids or bases are predicted from the drug pKa using the pH partitioning theory where pH_{ISF}, pH_{cyto} and pH_{lyso} are the pH values for brain ISF, intracellular cytosol and lysosomes, respectively:

$$K_{p,uu,cyto,base} = \frac{10^{pKa-pH_{cyto}} + 1}{10^{pKa-pH_{ISF}} + 1} \quad (11)$$

$$K_{p,uu,lyso,base} = \frac{10^{pKa-pH_{lyso}} + 1}{10^{pKa-pH_{cyto}} + 1} \quad (12)$$

$$K_{p,uu,cyto,acid} = \frac{10^{pH_{cyto}-pKa} + 1}{10^{pH_{ISF}-pKa} + 1} \quad (13)$$

$$K_{p,uu,lyso,acid} = \frac{10^{pH_{lyso}-pKa} + 1}{10^{pH_{cyto}-pKa} + 1} \quad (14)$$

Zwitterionic drugs have both acidic and basic functions. $K_{p,uu,cyto}$ and $K_{p,uu,lyso}$ were calculated as the product of the $K_{p,uu}$ values associated with the respective acid/base function. Values for $K_{p,uu}$ were similarly calculated for drugs with several acidic or basic functions (MacIntyre and Cutler, 1988). Accordingly, there is a separate model equation for each class of drugs. These equations are not given here due to space restrictions. However, a combined model equation that accommodates up to two acidic and two basic functions is provided as an Excel template spreadsheet (Supplemental Table 1).

Modelling of $K_{p,uu,cell}$

DMD Fast Forward. Published on December 13, 2010 as DOI: 10.1124/dmd.110.035998
This article has not been copyedited and formatted. The final version may differ from this version.

By assigning literature values to the parameters of the pH partition models, it is in principle possible to use the models directly to predict $K_{p,uu,cell}$ for conversion of $f_{u,brain}$ to $V_{u,brain}$. However, the strategy chosen was to "fine-tune" the model to provide the optimal prediction of $K_{p,uu,cell}$. This was done by fitting the models to experimental data on $K_{p,uu,cell}$, by including pH as a parameter in the model and thus estimating pH in the regression analysis. Modelling of the data also enabled an investigation of whether it is necessary to take into account partitioning into sub-cellular compartments (3-compartment model, Eq. 7) or whether a simpler model with a single intracellular compartment is sufficient (2-compartment model, Eq. 10). While pH_{cyto} and pH_{lyso} were the estimated parameters, fixed values were used for all other model parameters. The pH_{ISF} was set as 7.30, which is reported to be the physiological value (Davson and Segal, 1996) and is the same as the buffer pH in the slice method. V_{ISF} was taken as the physiological value 0.20 ml*g brain^{-1} (Nicholson and Sykova, 1998) and 0.01 ml*g brain^{-1} was used for V_{lyso}, rounded up from a value of 0.0068 reported for the liver (Weibel et al., 1969) since values were not available for brain tissue and because the cell contains acidic compartments in addition to lysosomes. Values of 0.79 ml*g brain^{-1} and 0.80 ml*g brain^{-1} were used for V_{cyto} in the 3-compartment and 2-compartment models, respectively. Physiological values were used as initial estimates for pH_{cyto} (7.02 (Friden et al., 2009a)) and for pH_{lyso} (5.0 (Ohkuma and Poole, 1978)).

Experimental data for $K_{p,uu,cell}$ were included for drugs with a single acidic or basic function and for one drug with two acidic functions (moxalactam). This was to ensure that the pH partition model was developed based only on compounds for which $K_{p,uu,cell}$ is primarily determined by pH partitioning.

Some compounds were not included in the model. The pKa of the basic function of metformin was too high to quantify using the employed methods (see measurement of pKa). Carrier-mediated transport of metformin was also suspected, based on prior information

DMD Fast Forward. Published on December 13, 2010 as DOI: 10.1124/dmd.110.035998
This article has not been copyedited and formatted. The final version may differ from this version.

(Kimura et al., 2005) and the deviating value of its $K_{p,uu,cell}$. Sulphasalazine had the lowest pKa (2.2) among the acids. It was considered an outlier because of the experimental value for $K_{p,uu,cell}$. Permanently cationic compounds and neutral drugs were not included since these are thought not to be influenced by pH partitioning. Zwitterionic drugs were similarly excluded, although minor effects are predicted depending on the pKa values. Compounds that were not used in the modeling are indicated by footnotes in Table 1.

For each of the two general models (the 2- and 3-compartment models), three functions were included in the construction of the regression model (WinNonlin® software; version 3.5) representing the pH partitioning of 1) monoprotic acids, 2) monoprotic bases and 3) the diprotic acid moxalactam. Simultaneous fitting of the three functions to the data results in a single set of parameter estimates for pH_{cyto} and pH_{lyso} (3-compartment model) or a single value for pH_{cyto} (2-compartment model). Goodness-of-fit was evaluated using the WinNonlin estimated precision of parameter estimates (coefficient of variation) and residual plot analysis. The 2- and 3-compartment models were compared by additionally calculating the Akaike Information Criterion (AIC) (Akaike, 1974).

Data presentation and statistical analysis

Aggregated $K_{p,uu,cell}$ values for compound classes are presented as means ± standard deviation. Values for $V_{u,brain}$ and $f_{u,brain}$ of single compounds are presented as means (standard error, SE). The SE for $V_{u,brain}$ was calculated for the 6 replicate slices. Since $f_{u,brain}$ is a single value which is scaled from the 3-5 replicate measurements of $f_{u,hD}$, it was necessary to use the propagation of error method (Kendall et al., 1987) to estimate SE for $f_{u,brain}$. This statistical approach estimates the standard error of $f_{u,brain}$ as a function of $f_{u,hD}$ (Eq. 13), using:

$$SE_{f_{u,brain}} = \sqrt{\left(\frac{\partial f_{u,brain}}{\partial f_{u,hD}}\right)^2 SE_{f_{u,hD}}^2} \qquad (15)$$

where $SE_{fu,brain}$ and $SE_{fu,hD}$ are the SE of the function $f_{u,brain}$ and the measurement $f_{u,hD}$. $\partial f_{u,brain}/\partial f_{u,hD}$ is the (partial) derivative of $f_{u,brain}$ with regard to $f_{u,hD}$, i.e. $\partial(f_{u,brain})/\partial(f_{u,hD})= D/\{(D-(D-1)*f_{u,hD})\text{^}2\}$, where D is the homogenate dilution factor.

The agreement of observed brain slice $V_{u,brain}$ values with predictions from $f_{u,brain}$ with or without using the pH partition model was evaluated according to the method of Altman and Bland (Bland and Altman, 1999). Since experimental variability appeared to be proportional to $V_{u,brain}$, i.e. the coefficient of variation was similar for compounds with very different $V_{u,brain}$ values, log-transformation of data was performed. The significance of a mean difference (bias) was tested with Student´s t test. The agreement between predicted and observed $V_{u,brain}$ values was expressed as the 95% confidence interval ratio (CIR) around the observed mean difference (bias), which was calculated using the t distribution. Owing to the log-transformation of data, the 95% confidence interval ranges from the mean difference divided by the 95% CIR to the mean difference multiplied by the 95% CIR.

DMD Fast Forward. Published on December 13, 2010 as DOI: 10.1124/dmd.110.035998
This article has not been copyedited and formatted. The final version may differ from this version.

Results

Overall comparison of brain slice $V_{u,brain}$ and homogenate $f_{u,brain}$

Brain slice $V_{u,brain}$ and brain homogenate $f_{u,brain}$ were inversely correlated (r^2 = 0.78), and $1/f_{u,brain}$ was within a three-fold range of $V_{u,brain}$ for 41 of the 56 compounds (Fig. 2A, Table 1). However, there were several compounds, including those subject to carrier-mediated transport, for which $V_{u,brain}$ was greatly underpredicted by $1/f_{u,brain}$. The $K_{p,uu,cell}$ factor, which provides the difference between the slice and homogenate methods for a drug (Eq. 4), was very high for MPP (77), metformin (9.5), TEA (9.0), paclitaxel (9.0), mitoxantrone (8.0) and gabapentin (4.6) (Fig. 2B). The $K_{p,uu,cell}$ results were clustered around 2.7 ± 0.6 for basic drugs carrying a single net positive charge at pH 7.4 (metformin excepted). Neutral drugs (paclitaxel excepted) and basic drugs that are predominantly neutral at pH 7.4 showed the smallest discrepancies between the methods ($K_{p,uu,cell}$ 0.99 ± 0.45). $K_{p,uu,cell}$ values for acidic drugs carrying a net negative charge at pH 7.4 were lower than unity (0.57 ± 0.18). After the acidic sulphasalazine ($K_{p,uu,cell}$ 0.27), moxalactam with two acidic functions had the lowest $K_{p,uu,cell}$ (0.46) in our dataset. $K_{p,uu,cell}$ values for zwitterions (gabapentin and mitoxantrone excluded) were close to unity (1.1 ± 0.47). Apart from MPP and TEA, as mentioned above, $K_{p,uu,cell}$ values for the permanently cationic compounds neostigmine and N-methylquinidine were 3.1 and 1.1, respectively.

The reproducibility of the results for the substantially bound quality control drug, propranolol, was slightly better for the slice than the homogenate method, as determined by the coefficient of variation (8% and 12%, respectively). For the whole data set it was observed that the slice method was consistently more precise than the homogenate method, irrespective of the degree of binding. In addition, the homogenate binding method was less precise at lower or no degrees of binding than at higher degrees of binding. The lower precision at low binding levels was shown statistically to result from the need to correct for brain homogenate dilution (Eqs. 3,

15, Fig 3B).

Modeling of pH partitioning

The clustering of $K_{p,uu,cell}$ values for drugs belonging to the same ion class, e.g. basic drugs, strongly suggested the involvement of pH partitioning in intra-brain distribution. The two pH partition models were fitted to the values of $K_{p,uu,cell}$ and pKa by estimation of intracellular pH_{cyto} alone (2-compartment model) or both pH_{cyto} and pH_{lyso} (3-compartment model). The 3-compartment model described the data better than the 2-compartment model as judged by the AIC values 8 and 33, respectively. Hence, it was necessary and appropriate to include the lysosomal sub-compartment. The fit of the 3-compartment model is shown in Fig. 4. The estimates (95% confidence intervals) for pH_{cyto} and pH_{lyso} were 7.06 (6.97-7.15) and 5.18 (5.06-5.29).

Using the 3-compartment model for $K_{p,uu,cell}$, $V_{u,brain}$ was predicted from $f_{u,brain}$ for all except the anticancer drugs (paclitaxel and mitoxantrone) and the permanently cationic drugs (Fig. 5). The 95% CIR for the agreement between observed and predicted $V_{u,brain}$ was 2.2 with no bias. This is to say that 95% of future predictions will fall within a 2.2-fold range of the observed values. Prediction of $V_{u,brain}$ by assuming that it equalled $1/f_{u,brain}$ resulted in a bias of 0.64-fold and a 4.5-fold 95% CIR. Hence, prediction of brain slice $V_{u,brain}$ using the homogenate $1/f_{u,brain}$ is associated with a 95% confidence interval between a 7.1-fold underprediction and a 2.9-fold overprediction.

Effect of lysosomal inhibition

To challenge the pH partition model, indomethacin (acid) and propranolol (base) were studied in brain slices while inhibiting the lysosomal pH gradient using increasing concentrations of monensin. There was slight acidification of the incubation buffer at the two higher monensin

DMD Fast Forward. Published on December 13, 2010 as DOI: 10.1124/dmd.110.035998
This article has not been copyedited and formatted. The final version may differ from this version.

concentrations (pH 7.16 and 7.02 for 5 and 50 nM monensin, respectively, versus pH 7.28 for lower monensin concentrations and the control). There was no effect on the intra-to-extracellular pH gradient (~0.2 pH units) except at 50 nM monensin, where the gradient was reduced to 0.08 pH units. $K_{p,uu,cell}$ for propranolol was reduced in a concentration-dependent manner across the whole range of monensin concentrations (50 pM to 50 nM), and was almost completely reduced to unity at the highest monensin concentrations (5 and 50 nM; Fig. 6). To assess the extent of lysosomal inhibition, the observed values for $K_{p,uu,cell}$ were compared with values predicted from the 3-compartment model, with measured values for pH_{ISF} and pH_{cyto} incorporated under the assumption of complete lysosomal inhibition ($pH_{lyso} = pH_{cyto}$). The agreement of predicted and observed propranolol $K_{p,uu,cell}$ at 5 and 50 nM monensin (Fig. 6) suggests that lysosomal trapping is nearly abolished at these concentrations.

The effect of monensin on indomethacin was different; there was no observed effect at any concentrations except the highest (50 nM). These results were consistent with the 3-compartment pH partition model which predicts that lysosomal inhibition will have no effect on the $K_{p,uu,cell}$ values of acidic drugs unless the overall pH gradient is also altered.

Inhibition of carrier-mediated organic cation transport

Inhibition of potential carrier-mediated uptake was studied for metformin and all permanently cationic drugs (MPP, TEA, , neostigmine and N-methylquinidine) using D22 concentrations ranging from 4 nM to 1 µM. Acidification of buffer and the intracellular space was seen at higher concentrations and the slices were significantly more swollen than control slices at 1 µM D22. There was little or no indication that the intra-to-extracellular pH gradient was altered by D22. $K_{p,uu,cell}$ was reduced for all compounds at 1 µM D22 (Fig. 7A). The effect was greatest for MPP (18-fold) and TEA (7-fold) followed by 2-fold reductions for metformin, neostigmine and N-methylquinidine. The transport of propranolol, which is supposedly not carrier-mediated and

DMD Fast Forward. Published on December 13, 2010 as DOI: 10.1124/dmd.110.035998
This article has not been copyedited and formatted. The final version may differ from this version.

was thus acting as a control, was reduced by a factor of 1.5. MPP behaved differently from the other compounds in that its much higher $K_{p,uu,cell}$ was also substantially reduced even at 0.2 µM D22, and that $K_{p,uu,cell}$ was slightly elevated at the lowest concentrations.

While the steady-state value for $V_{u,brain}$, and hence $K_{p,uu,cell}$, is generally expected to be reached after five hours' incubation (Friden et al., 2009a), it was seen for MPP, neostigmine and N-methyl quinidine (TEA was not studied) that $V_{u,brain}$ increased almost linearly from 1 hour to 5 hours (data not shown). Hence, values of $K_{p,uu,cell}$ for cationic drugs are not necessarily seen as steady-state values in this study.

Effect of lysosomal inhibition for permanent cations

There was no apparent effect of lysosomal inhibition by monensin on the uptake of metformin, N-methylquinidine, neostigmine or TEA. In contrast, the uptake of MPP was inhibited by monensin at concentrations similar to those required for inhibition of lysosomal trapping of propranolol (Fig. 7B). Inhibition of MPP uptake by monensin was more potent than that by D22.

Effect of active efflux inhibition

The $V_{u,brain}$ values of the Pgp substrates loperamide, saquinavir, nelfinavir and N-methylquinidine were not increased by the presence of 10 µM cyclosporine A (Fig. 8). Rather, cellular uptake of nelfinavir was reduced by cyclosporine A. The $V_{u,brain}$ values of the BCRP substrate mitoxantrone and the dual BCRP/MRP substrate sulphasalazine were also not increased in the presence of 10 µM fumitremorgin C, 20 µM MK-571 or both 10 µM fumitremorgin C and 20 µM MK-571.

Discussion

The distribution of drugs by cellular uptake within the brain can be studied in brain slices or in homogenized brain tissue. The primary interest in estimates of intra-brain distribution is their utility for converting measured total brain concentrations in vivo to pharmacologically active unbound drug concentrations. As the brain slice and brain homogenate methods are currently being used interchangeably for this purpose, the present study sought to identify, quantify and rationalize discrepancies between the methods in a dataset of 56 chemically diverse compounds exhibiting various mechanisms of distribution. Given the preserved cellular structure and viability of the brain slices, it is reasonable to assume that the brain slice $V_{u,brain}$ gives more information relevant to the in vivo situation than the homogenate method, which only measures non-specific binding. This was previously indicated in a study comparing results from the two methods with in vivo microdialysis results (Friden et al., 2007).

Nevertheless, the correlation (r^2 = 0.78) between $V_{u,brain}$ and $1/f_{u,brain}$ (Fig. 2) suggests that non-specific binding contributes as much as 78 % to the variations of $V_{u,brain}$ between drugs. The present study highlights another influential mechanism of drug distribution, namely pH partitioning. Much of the observed discrepancies between the methods were rationalized by the pH partition model, which accommodates the volumes and pH of the extra- and intracellular spaces and the intracellular lysosomal sub-compartment. The model, which predicts $K_{p,uu,cell}$, clearly explains how basic and acidic drugs accumulate in cells to a greater and lesser extent, respectively, than would be expected from non-specific binding. The model appears also to be applicable to compounds with more than a single basic or acidic function, since it was able to predict the very low value of $K_{p,uu,cell}$ for the diprotic acid moxalactam (Fig. 4).

Significant error is associated with using $f_{u,brain}$ and thereby assuming equivalence of the brain slice and homogenate methods ($V_{u,brain} = 1/f_{u,brain}$); the 95% confidence interval ranged from a 7.1-fold underprediction to a 2.9-fold overprediction. In contrast, using the pH

DMD Fast Forward. Published on December 13, 2010 as DOI: 10.1124/dmd.110.035998
This article has not been copyedited and formatted. The final version may differ from this version.

partition model with drug pKa values, it is possible to predict $V_{u,brain}$ with a 95% confidence interval ranging between 2.2-fold under- and overprediction. While it is preferable to measure the pKa values, it is recognized that the model is rather insensitive to pKa in the expected ranges for common carboxylic acids (pKa below 6) and amines (pKa above 8) (see Fig. 4). For many drugs it is therefore sufficient to use default $K_{p,uu,cell}$ values: ~3 for amines, ~0.6 for carboxylic acids, and 1 for neutral drugs or zwitterions.

The estimated pH values for lysosomes (pH_{lyso}=5.2) and cytosol (pH_{cyto}=7.1) were very similar to the physiological values and experimental measurements that were used as initial estimates. However, since all acidic sub-compartments have been included in the lysosomal compartment, the estimated pH values should primarily be seen as parameters describing drug distribution. The impact of pH partitioning on overall distribution was greater for basic drugs than for acidic and, obviously, neutral drugs. Because of the large pH difference (~2 units) between the cytosol and the lysosomes, the concentration of basic drugs is approximately 100 times higher in lysosomes than in the cytosol. This means that lysosomes represent nearly 50% of the total intracellular drug content in spite of their very small volume (~1% of the cell). In contrast, the lysosomal exclusion of acidic drugs has negligible impact on their overall distribution. The much smaller overall intra-to-extracellular pH gradient affects basic and acidic drugs to a similar extent but in opposite directions. Zwitterionic drugs are predicted to behave like neutral drugs, with small deviations depending on the exact pKa of the acidic or basic function. Moreover, the effect of lysosomal trapping, which is predicted from the model, was found to be in line with results from experiments where the lysosomal pH gradient was inhibited. The central role of pH partitioning in drug distribution, which has been demonstrated in this study in vitro, can be expected to translate to the in vivo situation. Early studies supporting this view showed that the in vivo tissue partition coefficients of various organs cannot be predicted for basic drugs using data from tissue homogenates (Schuhmann et al.,

1987, Harashima et al., 1984).

The highest observed values for $K_{p,uu,cell}$ were not predicted by the pH partition model. One of the compounds with a high $K_{p,uu,cell}$ was the zwitterionic gabapentin ($K_{p,uu,cell}$ = 4.5) which, although it was not bound non-specifically at all ($f_{u,brain}$ = 1), had a $V_{u,brain}$ of 4.5, indicating carrier-mediated active uptake. Gabapentin is known to be taken up into brain cells by the LAT1 transporter (Su et al., 1995). Intriguingly, the high $K_{p,uu,cell}$ indicates active uptake rather than facilitated uptake, which is the mode of transport for LAT1. Whatever the mechanism for gabapentin uptake, the brain slice $V_{u,brain}$ is very close to the value observed in vivo (5.5 mL*g brain^{-1} (Wang and Welty, 1996)).

The greatest discrepancy between the methods was seen for the permanently cationic prototypic OCT substrate MPP ($K_{p,uu,cell}$ = 77), which is also known to be taken up by the dopamine transporter in nigrostriatal nerve-end terminals. The slice uptake of MPP was potently inhibited by the OCT inhibitor D22, but even more potently inhibited by the lysosomal inhibitor monensin. This could be explained by the involvement of facilitated transport by OCT, secondary-active transport by a proton anti-porter, or effects on the sodium-driven dopamine transporter. The $K_{p,uu,cell}$ values for the other two model OCT substrates (metformin and TEA) were reduced by 1 µM D22 but not by monensin, suggesting no involvement of proton-coupled transport. As for LAT1, there should be no net transport of drug against an electrochemical gradient by the facilitating mode of OCT transport. TEA and MPP are, however, different from gabapentin in that they carry a permanent positive charge and are thus subject to the electric potential of the cell membrane. The Nernst equation predicts that a membrane potential of -60 mV results in an equilibrium chemical concentration gradient of ~10. Compared to most basic drugs, metformin may be particularly influenced by the electric potential, since its exceptionally high basic pKa makes it practically permanently charged.

There was no indication in the data that drug efflux by ABC transporters in the

parenchyma plays a significant role in limiting uptake into cells. The well characterized Pgp substrate loperamide seemed to be distributed intracellularly just like any other basic drug and $K_{p,uu,cell}$ was not increased by inhibition of Pgp. $V_{u,brain}$ of nelfinavir was unexpectedly reduced by cyclosporine A by an unidentified mechanism. Neither were there indications of drug efflux of the BCRP and MRP substrates mitoxantrone and sulphasalazine; there was no effect on mitoxantrone and $V_{u,brain}$ of sulphasalazine was paradoxically reduced. It appears likely that the expression level of ABC transporters in brain parenchyma is insufficient to produce significant efflux.

One important mechanism of distribution which has not been considered so far involves specific binding to the target protein of the drug. The contribution of specific binding to the overall distribution can be anticipated to be highly dependent on the level of expression of the target protein. It is speculated that the very large $K_{p,uu,cell}$ for the two anti-cancer drugs paclitaxel (9.0) and mitoxantrone (8.0) could be somehow related to specific binding to tubulin and DNA, respectively, which exist at much higher molar concentrations than most target receptors, enzymes and transporters. In fact, accumulation of paclitaxel in platelets is known to be saturable (Wild et al., 1995).

The pharmacological significance of intra-brain and intracellular distribution is currently not as clear as that of BBB transport. However, the concepts discussed in the present paper are relevant to intracellular drug targeting not only in brain but also in other organs; for the same unbound drug concentration in the extracellular fluid, the intracellular exposure will be slightly higher for basic drugs and lower for acidic drugs. Furthermore, by measuring both non-specific binding (homogenate) and overall uptake (slice), the calculated $K_{p,uu,cell}$ may provide insight into the intracellular exposure to unbound drug and the involvement of active uptake.

In conclusion, drug distribution within brain tissue occurs by a variety of processes

including non-specific and specific binding, pH partitioning across the cell membrane and the membranes of intracellular lysosomes, and carrier-mediated uptake driven by chemical gradients, membrane potential and possibly pH gradients. It was also indirectly demonstrated that these physiological mechanisms are intact in the brain slices and that the slice method therefore has the potential to capture these mechanisms when estimating intra-brain drug distribution. Apart from being closer to the in vivo situation, and therefore providing more accurate values of intra-brain distribution, the data from the slice method were also associated with higher and more consistent precision for both extensively and poorly binding drugs. If the homogenate method is used as an alternative for estimation of intra-brain drug distribution, the bias associated with acids and bases should be corrected for by using the proposed pH partition model for $K_{p,uu,cell}$. This correction is carried out by dividing the calculated $K_{p,uu,cell}$ by the measured value of $f_{u,brain}$, yielding an estimated value for $V_{u,brain}$, or equivalently, by dividing $f_{u,brain}$ by $K_{p,uu,cell}$, yielding a value for $f_{u,brain}$ more relevant to the in vivo situation.

Authorship Contribution

Participated in research design: Fridén, Bergström, Wan, Rehngren, Ahlin, Hammarlund-Udenaes, and Bredberg

Conducted experiments: Fridén, Bergström, Wan and Rehngren

Performed data analysis: Fridén, Bergström, Wan and Rehngren

Wrote or contributed to the writing of the manuscript: Fridén, Bergström, Wan, Rehngren, Ahlin, Hammarlund-Udenaes, and Bredberg

References

Akaike H. (1974) A new look at the statistical model identification. *IEEE Transactions on Automatic Control*.

Bland JM and Altman DG. (1999) Measuring agreement in method comparison studies.[see comment]. *Stat Methods Med Res* **8**:135-160.

Bleasby K, Castle JC, Roberts CJ, Cheng C, Bailey WJ, Sina JF, Kulkarni AV, Hafey MJ, Evers R, Johnson JM, Ulrich RG, and Slatter JG. (2006) Expression profiles of 50 xenobiotic transporter genes in humans and pre-clinical species: a resource for investigations into drug disposition. *Xenobiotica* **36**:963-988.

Dallas S, Miller DS, and Bendayan R. (2006) Multidrug resistance-associated proteins: Expression and function in the central nervous system. *Pharmacol Rev* **58**:140-161.

Daniel WA, Bickel MH, and Honegger UE. (1995) The contribution of lysosomal trapping in the uptake of desipramine and chloroquine by different tissues. *Pharmacol Toxicol* **77**:402-406.

Davson H and Segal MB. (1996) Acid-base relations in the central nervous system, in *Physiology of the CSF and Blood-Brain Barriers*(Anonymous) pp 459-488, CRC Press, Boca Raton.

de Duve C, de Barsy T, Poole B, Trouet A, Tulkens P, and Van Hoof F. (1974) Commentary. Lysosomotropic agents. *Biochem Pharmacol* **23**:2495-2531.

Friden M, Gupta A, Antonsson M, Bredberg U, and Hammarlund-Udenaes M. (2007) In vitro methods for estimating unbound drug concentrations in the brain interstitial and intracellular fluids. *Drug Metabolism & Disposition* **35**:1711-1719.

Friden M, Ducrozet F, Antonsson M, Middleton B, Bredberg U, and Hammarlund-Udenaes M. (2009a) Development of a high-throughput brain slice method for studying drug distribution in the CNS. *Drug Metab Dispos* **37**:1226.

Friden M, Winiwarter S, Jerndal G, Bengtsson O, Wan H, Bredberg U, Hammarlund-Udenaes M, and Antonsson M. (2009b) Structure-brain exposure relationships in rat and human using a novel data set of unbound drug concentrations in brain interstitial and cerebrospinal fluids. *J Med Chem* **52**:6233-6243.

Gorboulev V, Ulzheimer JC, Akhoundova A, Ulzheimer-Teuber I, Karbach U, Quester S, Baumann C, Lang F, Busch AE, and Koepsell H. (1997) Cloning and characterization of two human polyspecific organic cation transporters. *DNA Cell Biol* **16**:871-881.

Grundemann D, Schechinger B, Rappold GA, and Schomig E. (1998) Molecular identification of the corticosterone-sensitive extraneuronal catecholamine transporter. *Nat Neurosci* **1**:349-351.

Harashima H, Sugiyama Y, Sawada Y, Iga T, and Hanano M. (1984) Comparison between in-vivo and in-vitro tissue-to-plasma unbound concentration ratios (Kp,f) of quinidine in rats. *J Pharm Pharmacol* **36**:340-342.

Kakee A, Terasaki T, and Sugiyama Y. (1996) Brain efflux index as a novel method of analyzing efflux transport at the blood-brain barrier. *Journal of Pharmacology & Experimental Therapeutics* **277**:1550-1559.

Kalvass JC and Maurer TS. (2002) Influence of nonspecific brain and plasma binding on CNS exposure: implications for rational drug discovery. *Biopharm Drug Dispos* **23**:327-338.

Kendall M, Stuart A, and Ord K. (1987) *Advanced Theory of Statistics*, Hodder Arnold, London.

Kimura N, Masuda S, Tanihara Y, Ueo H, Okuda M, Katsura T, and Inui K. (2005) Metformin is a superior substrate for renal organic cation transporter OCT2 rather than hepatic OCT1. *Drug Metab Pharmacokinet* **20:**379-386.

Lake JR, Van Dyke RW, and Scharschmidt BF. (1987) Acidic vesicles in cultured rat hepatocytes. Identification and characterization of their relationship to lysosomes and other storage vesicles. *Gastroenterology* **92**:1251-1261.

Liu X, Van Natta K, Yeo H, Vilenski O, Weller PE, Worboys PD, and Monshouwer M. (2009) Unbound drug concentration in brain homogenate and cerebral spinal fluid at steady state as a surrogate for unbound concentration in brain interstitial fluid. *Drug Metab Dispos* **37**:787-793.

MacIntyre AC and Cutler DJ. (1988) The potential role of lysosomes in tissue distribution of weak bases. *Biopharm Drug Dispos* **9**:513-526.

Mano Y, Higuchi S, and Kamimura H. (2002) Investigation of the high partition of YM992, a novel antidepressant, in rat brain - in vitro and in vivo evidence for the high binding in brain and the high permeability at the BBB. *Biopharmaceutics & Drug Disposition.* **23**:351-360.

Nicholson C and Sykova E. (1998) Extracellular space structure revealed by diffusion analysis.[see comment]. *Trends Neurosci* **21**:207-215.

Ohkuma S and Poole B. (1978) Fluorescence probe measurement of the intralysosomal pH in living cells and the perturbation of pH by various agents. *Proc Natl Acad Sci U S A* **75**:3327-3331.

Schuhmann G, Fichtl B, and Kurz H. (1987) Prediction of drug distribution in vivo on the basis of in vitro binding data. *Biopharm Drug Dispos* **8**:73-86.

Shore PA, Brodie BB, and Hogben CA. (1957) The gastric secretion of drugs: a pH partition hypothesis. *J Pharmacol Exp Ther* **119**:361-369.

Siebert GA, Hung DY, Chang P, and Roberts MS. (2004) Ion-trapping, microsomal binding, and unbound drug distribution in the hepatic retention of basic drugs. *J Pharmacol Exp Ther* **308**:228-235.

Su TZ, Lunney E, Campbell G, and Oxender DL. (1995) Transport of gabapentin, a gamma-amino acid drug, by system l alpha-amino acid transporters: a comparative study in astrocytes, synaptosomes, and CHO cells. *J Neurochem* **64**:2125-2131.

Waddell WJ and Butler TC. (1959) Calculation of intracellular pH from the distribution of 5,5-dimethyl-2,4-oxazolidinedione (DMO); application to skeletal muscle of the dog. *J Clin Invest* **38**:720-729.

Wan H and Ulander J. (2006) High-throughput pKa screening and prediction amenable for ADME profiling. *Expert Opin Drug Metab Toxicol* **2**:139-155.

Wan H, Rehngren M, Giordanetto F, Bergstrom F, and Tunek A. (2007) High-throughput screening of drug-brain tissue binding and in silico prediction for assessment of central nervous system drug delivery. *J Med Chem* **50**:4606-4615.

Wan H, Holmen AG, Wang Y, Lindberg W, Englund M, Nagard MB, and Thompson RA. (2003) High-throughput screening of pKa values of pharmaceuticals by pressure-assisted capillary electrophoresis and mass spectrometry. *Rapid Commun Mass Spectrom* **17**:2639-2648.

Wang Q, Strab R, Kardos P, Ferguson C, Li J, Owen A, and Hidalgo IJ. (2008) Application and limitation of inhibitors in drug-transporter interactions studies. *Int J Pharm* **356**:12-18.

Wang Y and Welty DF. (1996) The simultaneous estimation of the influx and efflux blood-brain barrier permeabilities of gabapentin using a microdialysis-pharmacokinetic approach. *Pharm Res* **13**:398-403.

Weibel ER, Staubli W, Gnagi HR, and Hess FA. (1969) Correlated morphometric and biochemical studies on the liver cell. I. Morphometric model, stereologic methods, and normal morphometric data for rat liver. *J Cell Biol* **42**:68-91.

Wild MD, Walle UK, and Walle T. (1995) Extensive and saturable accumulation of paclitaxel by the human platelet. *Cancer Chemother Pharmacol* **36**:41-44.

Legends for figures

Figure 1. Schematic representation of the pH partitioning of acidic and basic drugs between the ISF of the extracellular space, the intracellular cytosol and the acidic intracellular sub-compartments (denoted lysosomes). The concentrations of the non-ionized species of acidic (HA) and basic (B) drugs are equal in all compartments at equilibrium and governed by the concentrations in ISF. HA and B are also in equilibrium with their ionized counterparts A^- and HB^+, respectively, in each compartment. This equilibrium is shifted in acidic intracellular compartments (rich in protons, H^+) towards the protonated forms HA and HB^+, respectively, such that A^- is depleted and HB^+ is elevated.

Figure 2. Relationship between (A) $1/f_{u,brain}$ determined using the brain homogenate method and $V_{u,brain}$ determined using the slice method and (B) $K_{p,uu,cell}$ plotted against $1/f_{u,brain}$. In A, the solid and dotted lines represent agreement and a 3-fold difference. In B, the solid and dotted lines represent $K_{p,uu,cell}$ = 1, 3 and 1/3, respectively. Compounds are classified as acids, bases, zwitterions, neutrals and permanent cations, based on the predominant ionization state at pH 7.4.

Figure 3. Plot of the relative standard error (RSE) for (A) $f_{u,brain}$ (homogenate method) and $V_{u,brain}$ (slice method) versus $f_{u,brain}$, and (B) simulated RSE for $f_{u,brain}$, given an arbitrary 5% RSE for $f_{u,hD}$, showing an estimated increase in RSE of the homogenate method with increasing $f_{u,brain}$.

Figure 4. The fit of the 3-compartment pH partition model (Eq. 7) to experimental data on $K_{p,uu,cell}$ for drugs with a single basic function (gray solid line), drugs with a single acidic

DMD Fast Forward. Published on December 13, 2010 as DOI: 10.1124/dmd.110.035998
This article has not been copyedited and formatted. The final version may differ from this version.

function (black solid line) and a drug with a dual acidic function (dashed line). Several drugs in the figure with a basic or acidic function are classified as neutrals in Table 1 and Fig. 2 based on the predominant charge at pH 7.4. Three drugs (midazolam, nelfinavir and saquinavir) with pKa of the basic functions ranging from 5.4 to 6.8 behaved more as acids due for an unknown reason.

Figure 5. Plot of predicted versus observed values for $V_{u,brain}$ in slices, using the homogenate $f_{u,brain}$ alone (filled grey circles) or in combination with the pH partition model for $K_{p,uu,cell}$ (solid black circles). Predictions were not made for the anticancer drugs (paclitaxel and mitoxantrone) or the permanently cationic drugs.

Figure 6. Effect of lysosomal inhibition by monensin on $K_{p,uu,cell}$ for a prototypic basic drug (propranolol) and a prototypic acidic drug (indomethacin). Markers connected by solid lines represent observed values. Markers connected by dashed lines represent predicted values from the 3-compartment pH partition model, based on the assumption that lysosomes are completely inhibited ($pH_{lyso} = pH_{cyto}$), and on the incorporation of measured values for pH_{ISF} (buffer pH) and pH_{cyto} (intracellular pH). The lack of agreement between observed and predicted values for propranolol at lower monensin concentrations indicates the existence of a drug accumulation process in addition to non-specific binding and pH partitioning across the cell membrane i.e. lysosomal trapping. The convergence of observed and predicted values at higher monensin concentrations suggests complete lysosomal inhibition. The agreement of observed and predicted values for indomethacin suggests that its cellular accumulation is sufficiently explained by non-specific binding and pH-partitioning across the cell membrane.

Figure 7. Effect of D22 (OCT inhibition, A) and monensin (lysosomal inhibition, B) on the

$K_{p,uu,cell}$ of permanently cationic compounds and metformin. Error bars represent the SE for 6 slices. Propranolol is included as reference.

Figure 8. The effect of cyclosporine A (Pgp inhibition, A) and FTC and MK-571 (inhibition of BCRP and MRP, B) on the $V_{u,brain}$ of selected substrates. Error bars represent the SE for 6 slices.

DMD Fast Forward. Published on December 13, 2010 as DOI: 10.1124/dmd.110.035998
This article has not been copyedited and formatted. The final version may differ from this version.

Tables

Table 1. Experimentally determined values for pKa, brain homogenate $f_{u,brain}$ and brain slice $V_{u,brain}$. Values for $K_{p,uu,cell}$ are calculated from $f_{u,brain}$ and $V_{u,brain}$ (Observed) and predicted from the pH partition model (Predicted). Ion class refers to acid base properties which are most relevant at the physiological pH 7.4. Hence, drugs with a basic pKa below 7.4 and drugs with acidic pKa above 7.4 are termed neutral.

Compound	pKa		Ion class	$f_{u,brain}$	$V_{u,brain}$	$K_{p,uu,cell}$	
	Acid	Base			ml* g brain^{-1}	Observed	Predicted
Alprazolam		2.4	Neutral	0.16 (0.034)	6.5 (0.17)	1.07	1
Alprenolol		9.7	Base	0.057 (0.0013)	50 (1.3)	2.83	2.89
Amantadine		10.8	Base	0.29 (0.052)	9.9 (0.23)	2.83	2.90
Amitriptyline		9.5	Base	0.010 (0.0005)	310 (13)	3.08	2.89
Atenolol		9.7	Base	0.90 (0.052)	2.5 (0.05)	2.25	2.89
Baclofen[a]	3.7	9.7	Zwitterion	0.98 (0.083)	1.7 (0.05)	1.62	1
Bupropion		8.6	Base	0.17 (0.012)	16 (0.13)	2.66	2.80
Cimetidine		7.0	Neutral	0.76 (0.027)	2.3 (0.03)	1.73	1.63
Clonidine		8.3	Base	0.42 (0.035)	5.9 (0.42)	2.47	2.71
Codeine		8.4	Base	0.62 (0.037)	3.2 (0.08)	1.99	2.76
Delaviridine		4.5	Neutral	0.022 (0.0013)	40 (1.3)	0.86	1
Diazepam		3.6	Neutral	0.041 (0.0046)	20 (0.17)	0.80	1
Diclophenac	4		Acid	0.041 (0.0044)	15 (0.35)	0.61	0.65
Diphenhydramine		9.3	Base	0.093 (0.015)	32 (0.31)	3.02	2.88
Ethyl-2-Phenylmalonamide			Neutral	0.65 (0.1)	0.93 (0.04)	0.60	1
Fluorescein	5.2		Acid	0.42 (0.061)	1.8 (0.06)	0.74	0.66
Gabapentin[a]	3.9	10.5	Zwitterion	1.06 (0.075)	4.6 (0.13)	4.55[d]	1
Indomethacin	4.1		Acid	0.044 (0.0047)	14 (0.27)	0.60	0.65
Lamotrigine		5.2	Neutral	0.21 (0.0089)	4.6 (0.14)	0.96	1.01

DMD Fast Forward. Published on December 13, 2010 as DOI: 10.1124/dmd.110.035998
This article has not been copyedited and formatted. The final version may differ from this version.

Levofloxacin[a]	6.0	8.5	Zwitterion	0.84 (0.017)	1.7 (0.03)	1.44	1.07
Loperamide		9	Base	0.0080 (0.0002)	370 (3.5)	2.95	2.86
M3G[a]	3.1	8.5	Zwitterion	0.97 (0.067)	0.60 (0.03)	0.58	0.98
M6G[a]	4.3	9	Zwitterion	0.87 (0.094)	0.98 (0.03)	0.86	1
Metformin		>11	Base	0.95 (0.17)	10 (0.3)	9.51	2.90
Methotrexate[a]	3.1	5.4	Zwitterion	0.89 (0.044)	0.68 (0.03)	0.61	0.66
Metoprolol		9.7	Base	0.46 (0.053)	5.5 (0.13)	2.53	2.89
Midazolam		5.4	Neutral	0.026 (0.0013)	29 (0.75)	0.74	1.02
Mitoxantrone[a,b]	3.2	8.4[c]	Zwitterion	0.0046 (0.0004)	1757 (23)	8.01	2.67
Morphine		8.3	Base	0.76 (0.052)	3.7 (0.07)	2.81	2.73
Moxalactam	2.9[c]		Acid	12 (19)	0.46 (0.04)	0.46[d]	0.46
MPP+[a,b]			Cation	0.49 (0.025)	157 (0.85)	77	1
Nadolol		9.9	Base	0.78 (0.027)	3.4 (0.12)	2.63	2.90
Nelfinavir		6.3	Neutral	0.00072 (0.00005)	860 (21)	0.62	1.16
Neostigmine[a,b]		19.1	Cation	0.95 (0.3)	3.2 (0.05)	3.07	2.90
N-methyl quinidine[a,b]			Cation	0.23 (0.059)	4.6 (0.09)	1.06	1
Norfloxacin[a]	4.4	8.7	Zwitterion	0.58 (0.057)	2.9 (0.14)	1.66	0.99
Oxprenolol		9.7	Base	0.28 (0.02)	11.8 (0.16)	3.25	2.89
Oxycodone		9.1	Base	0.66 (0.025)	4.2 (0.13)	2.78	2.87
Oxymorphone		8.7	Base	0.75 (0.053)	4.0 (0.12)	2.97	2.82
Paclitaxel[a,b]			Neutral	0.012 (0.0006)	769 (27)	9.03	1
Pindolol		9.7	Base	0.40 (0.005)	7.2 (0.12)	2.89	2.89
Propranolol		9.6	Base	0.029 (0.0008)	112 (1)	3.29	2.89
Quinidine		8.8	Base	0.09 (0.0052)	38 (0.6)	3.45	2.84
Quinine		8.8	Base	0.082 (0.0042)	43 (0.51)	3.51	2.84
Rifampicin[a]	2.2	7.6	Zwitterion	0.13 (0.0046)	6.9 (0.14)	0.92	0.88
Salicylic acid	4.3		Acid	0.63 (0.046)	1.0 (0.09)	0.62	0.66
Saquinavir		6.8	Neutral	0.0038 (0.0004)	208 (0.8)	0.79	1.49
Sulphasalazine	2.0		Acid	0.063 (0.0022)	4.2 (0.36)	0.27	0.65
Tacrine		10	Base	0.16 (0.01)	22 (0.59)	3.5	2.9

TEA[a,b]			Cation	1.0 (0.078)	9.0 (0.1)	8.95	1
Thiopental	7.6		Neutral	0.16 (0.0087)	4.3 (0.67)	0.67	0.88
Thioridazine		8.9	Base	0.00067 (0.00003)	3333 (68)	2.24	2.86
Topiramate			Neutral	0.61 (0.063)	3.2 (0.08)	1.96	1
Tramadol		9.7	Base	0.53 (0.046)	4.2 (0.07)	2.25	2.89
Verapamil		8.9	Base	0.052 (0.0019)	54 (1.4)	2.81	2.86
Zidovudine			Neutral	0.95 (0.018)	1.1 (0.03)	1.08	1

a, Not used for deriving the pH partition model.

b, Not included when evaluating the predictivity of the pH partition model.

c, Double acidic or basic function.

d, Calculated using $f_{u,brain}$=1.0 .

DMD Fast Forward. Published on December 13, 2010 as DOI: 10.1124/dmd.110.035998
This article has not been copyedited and formatted. The final version may differ from this version.

Fig 1

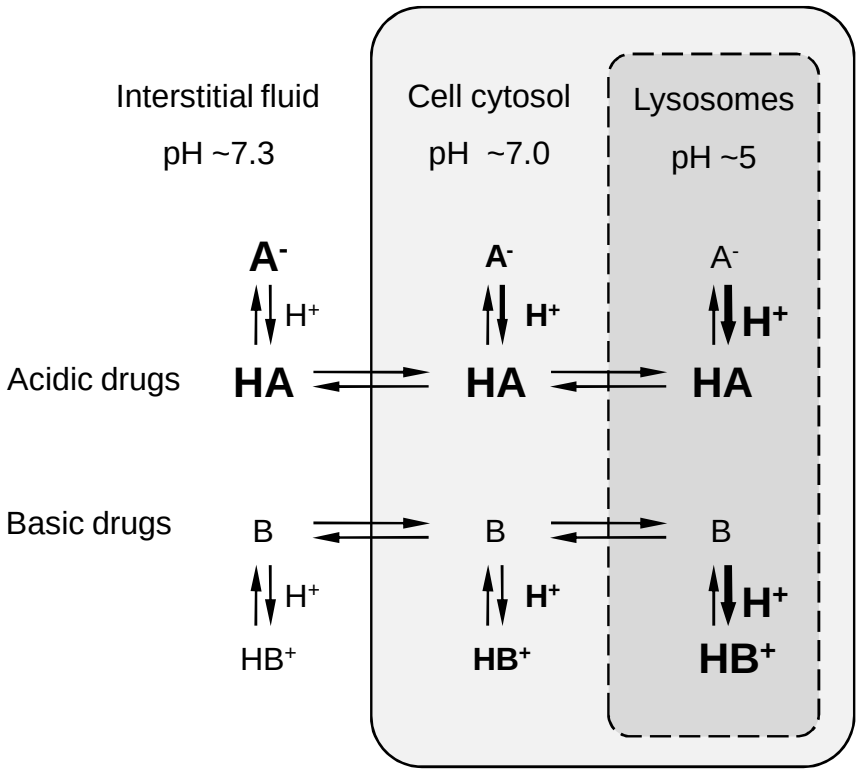

Fig 2

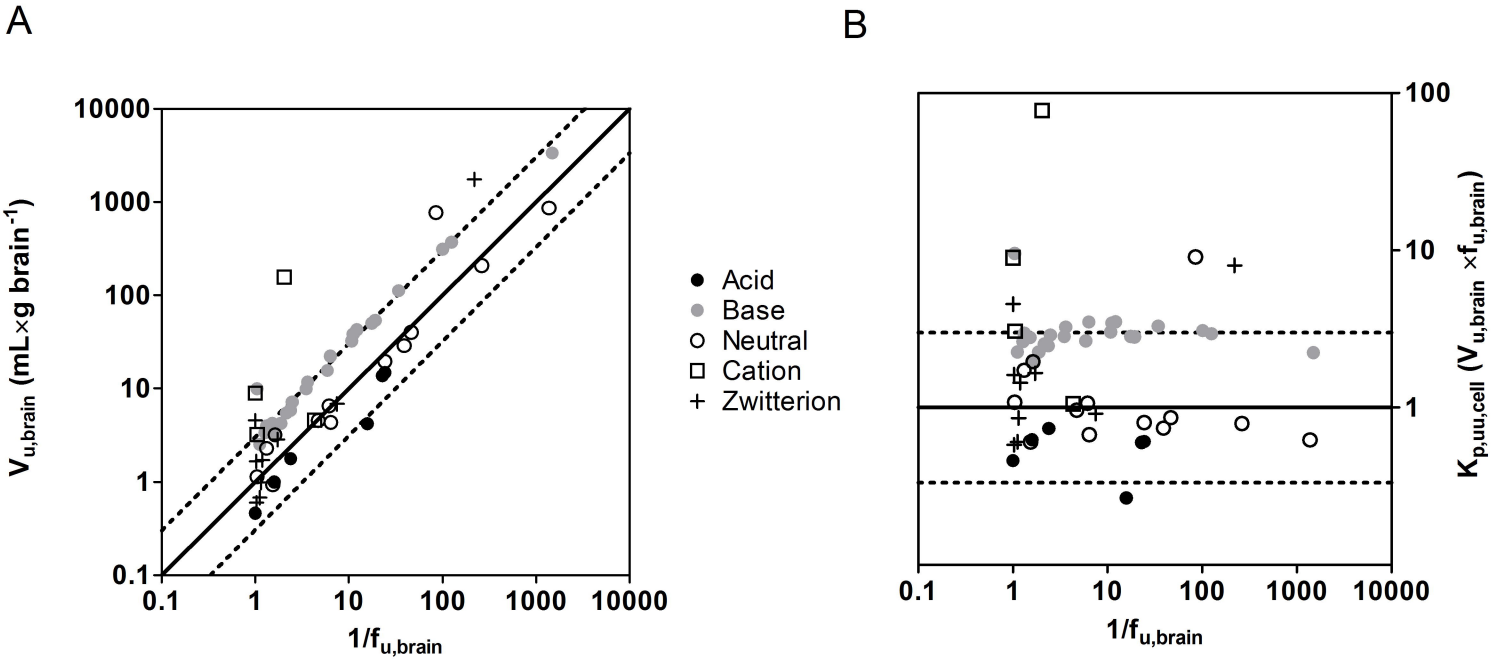
A
B
10000
1000
100
10
1
0.1
0.1
1
10
100
1000
10000
$V_{u,brain}$ (mL×g brain^{-1})
$1/f_{u,brain}$
Acid
Base
Neutral
Cation
Zwitterion
100
10
1
$K_{p,uu,cell}$ ($V_{u,brain}$ ×$f_{u,brain}$)

Fig 3

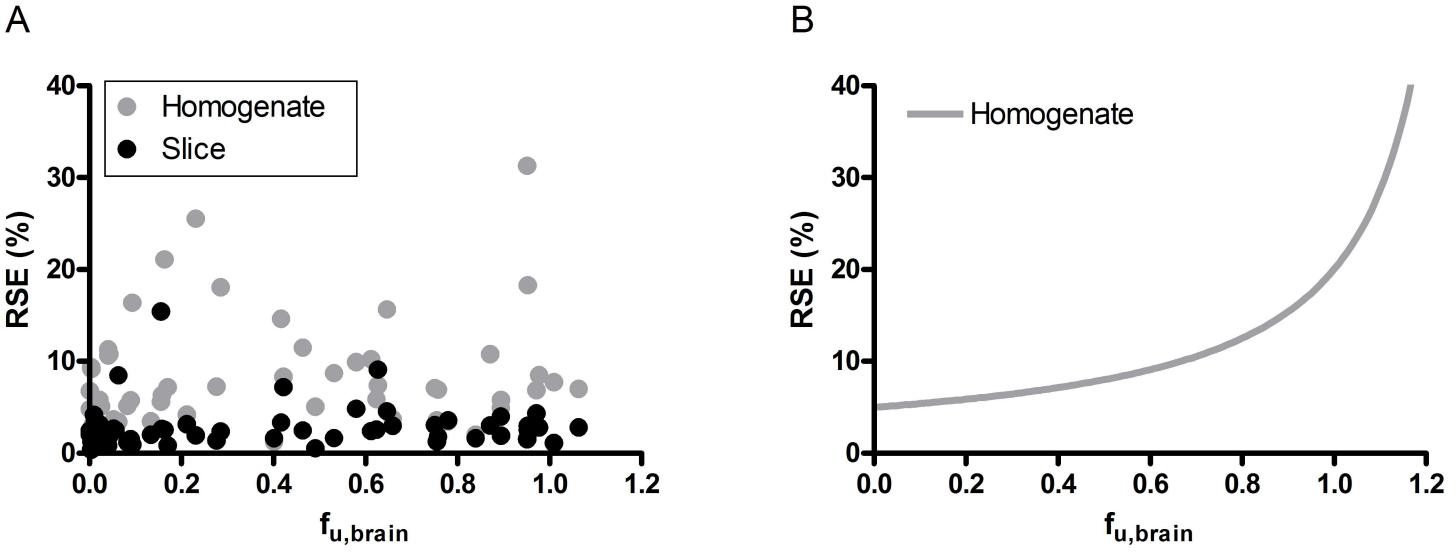
A
Homogenate
Slice
RSE (%)
40
30
20
10
0
0.0
0.2
0.4
0.6
0.8
1.0
1.2
$f_{u,brain}$
B
Homogenate
RSE (%)
40
30
20
10
0
0.0
0.2
0.4
0.6
0.8
1.0
1.2
$f_{u,brain}$

Fig 4

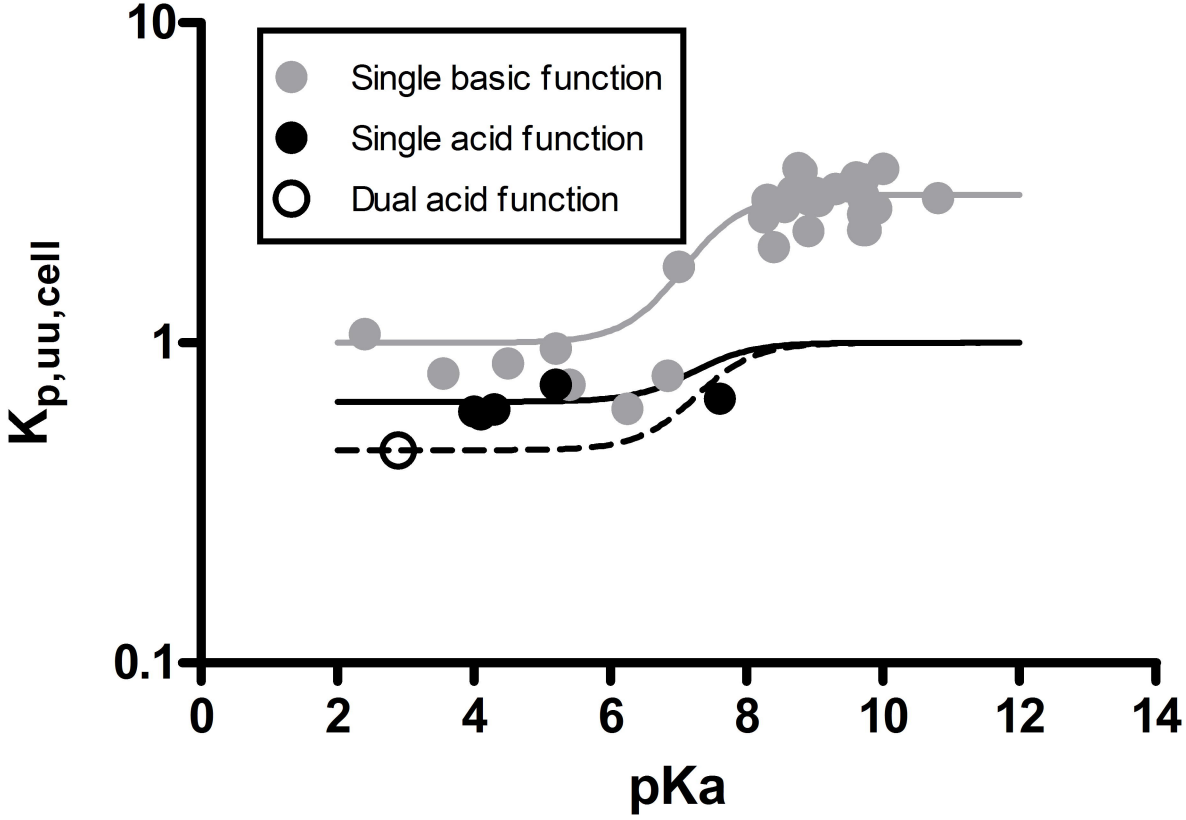
10
1
0.1
$K_{p,uu,cell}$
Single basic function
Single acid function
Dual acid function
0
2
4
6
8
10
12
14
pKa

Fig 5

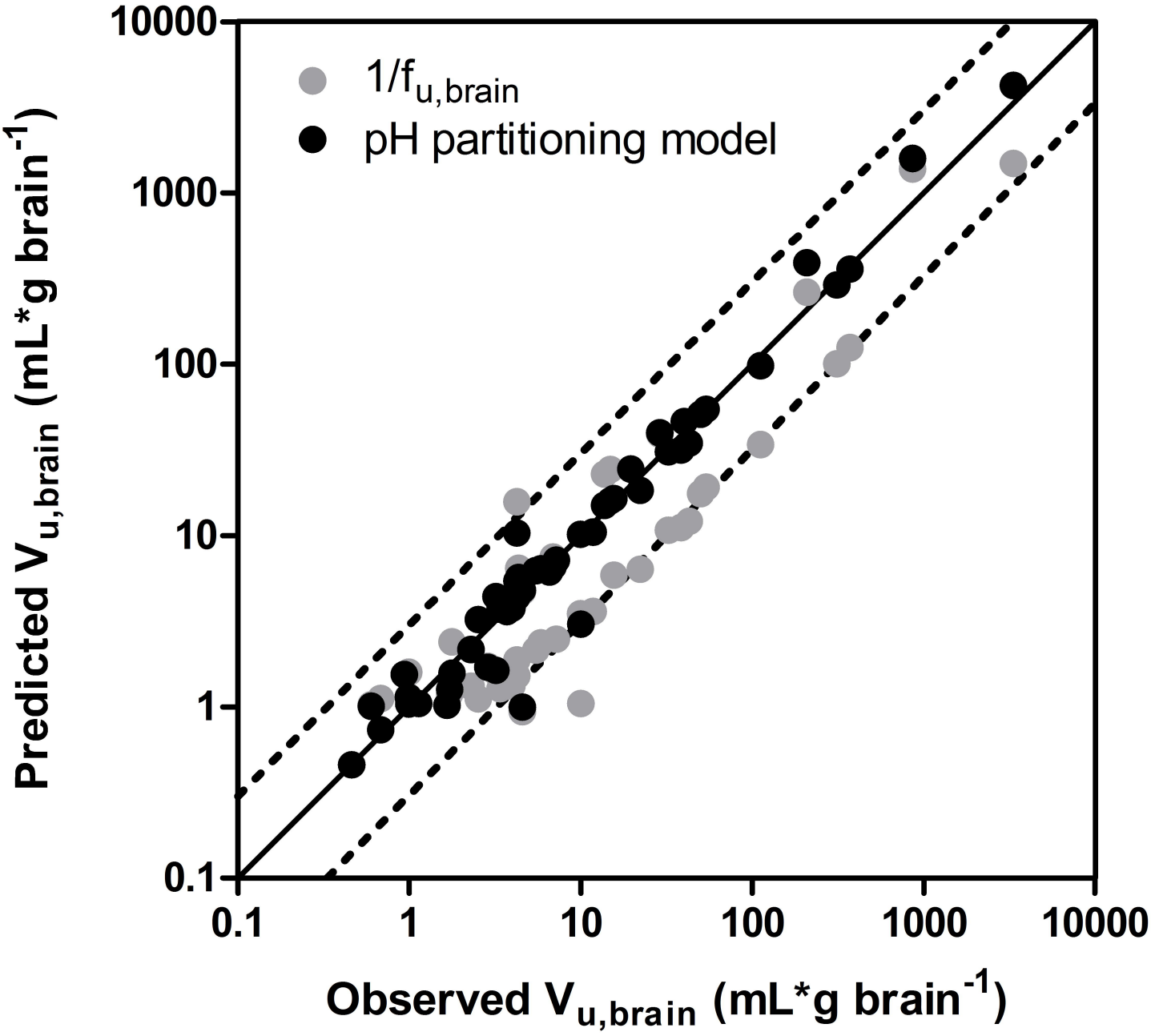
10000
1000
100
10
1
0.1
0.1
1
10
100
1000
10000
1/f u,brain
pH partitioning model
Predicted V u,brain (mL*g brain -1)
Observed V u,brain (mL*g brain -1)

Fig 6

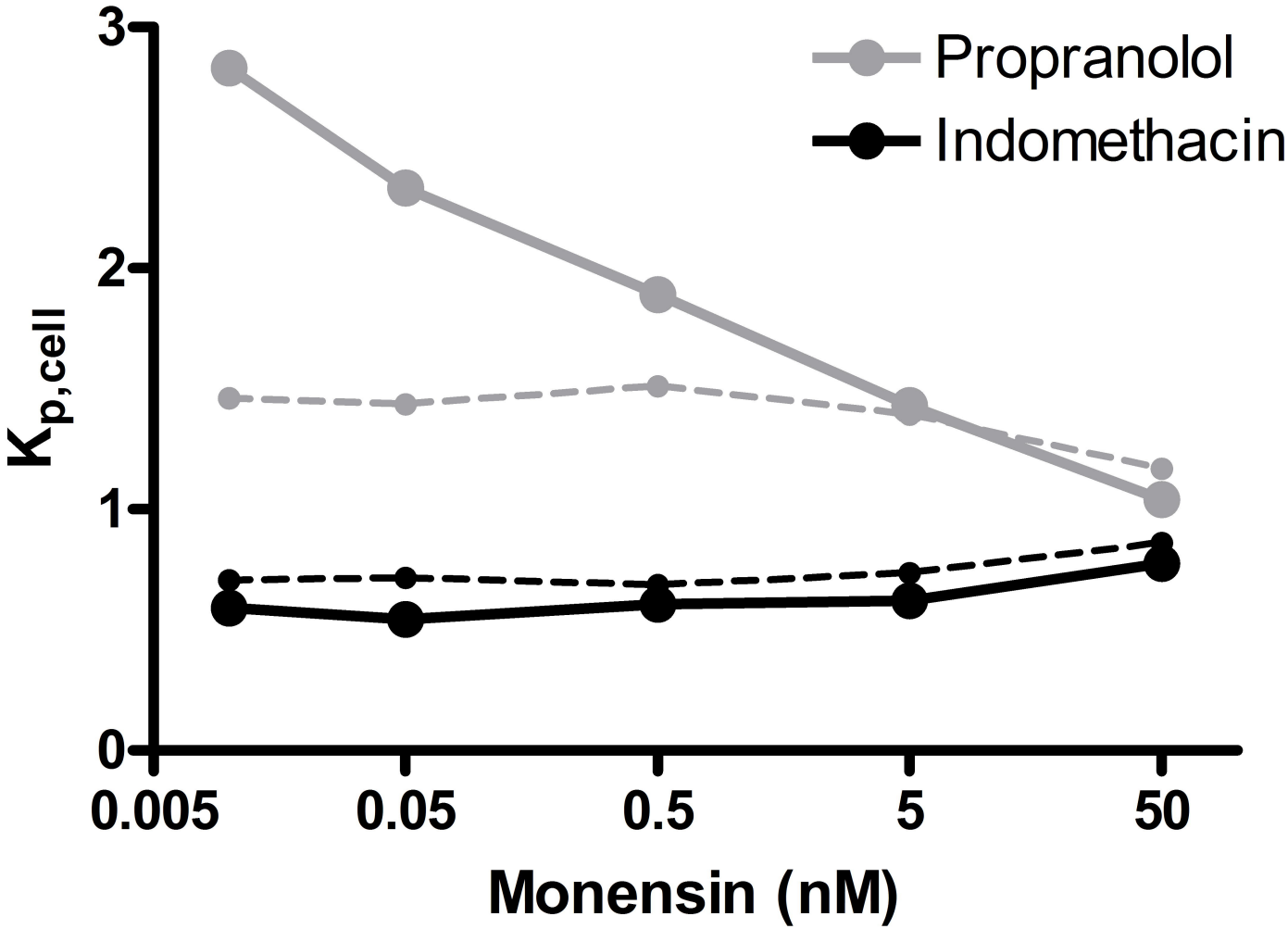
Propranolol
Indomethacin
$K_{p,cell}$
3
2
1
0
0.005
0.05
0.5
5
50
Monensin (nM)

Fig 7

A

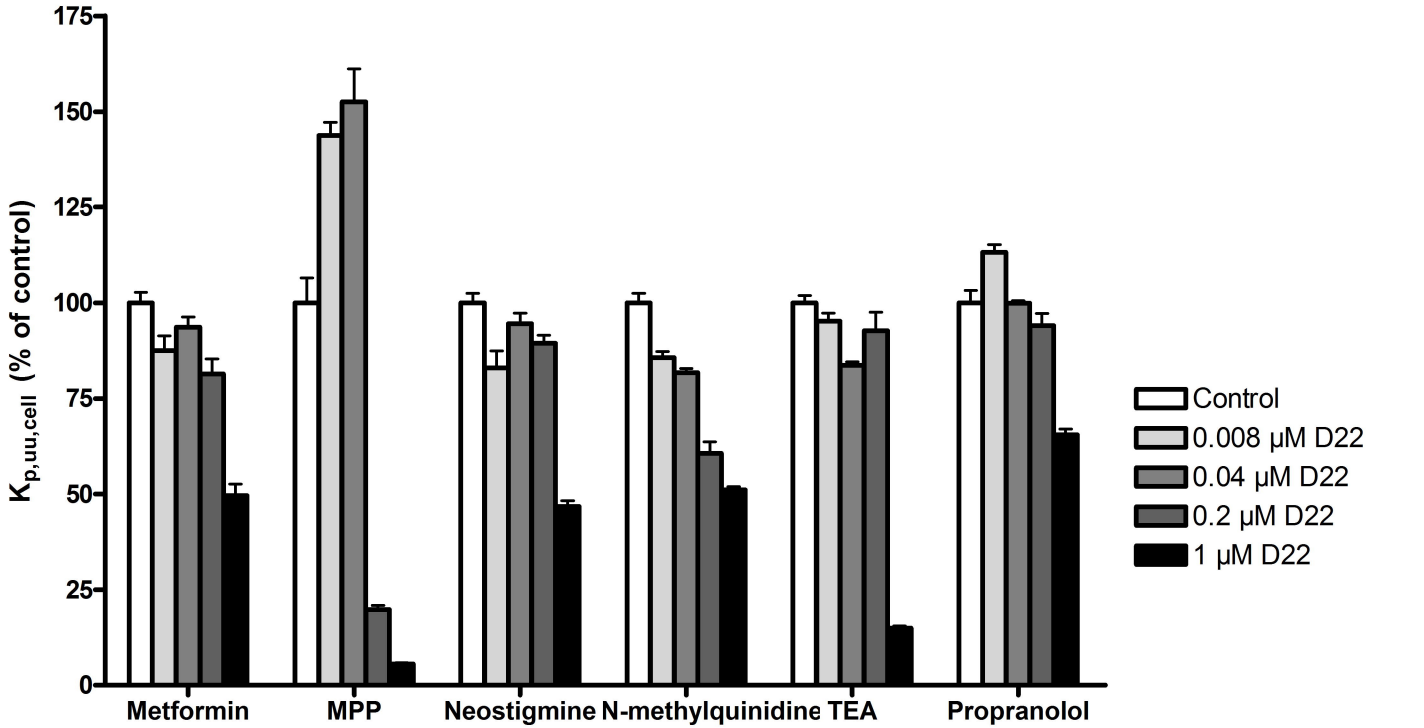
175
150
125
100
75
50
25
0
$K_{p,uu,cell}$ (% of control)
Metformin
MPP
Neostigmine
N-methylquinidine
TEA
Propranolol
Control
0.008 µM D22
0.04 µM D22
0.2 µM D22
1 µM D22

B

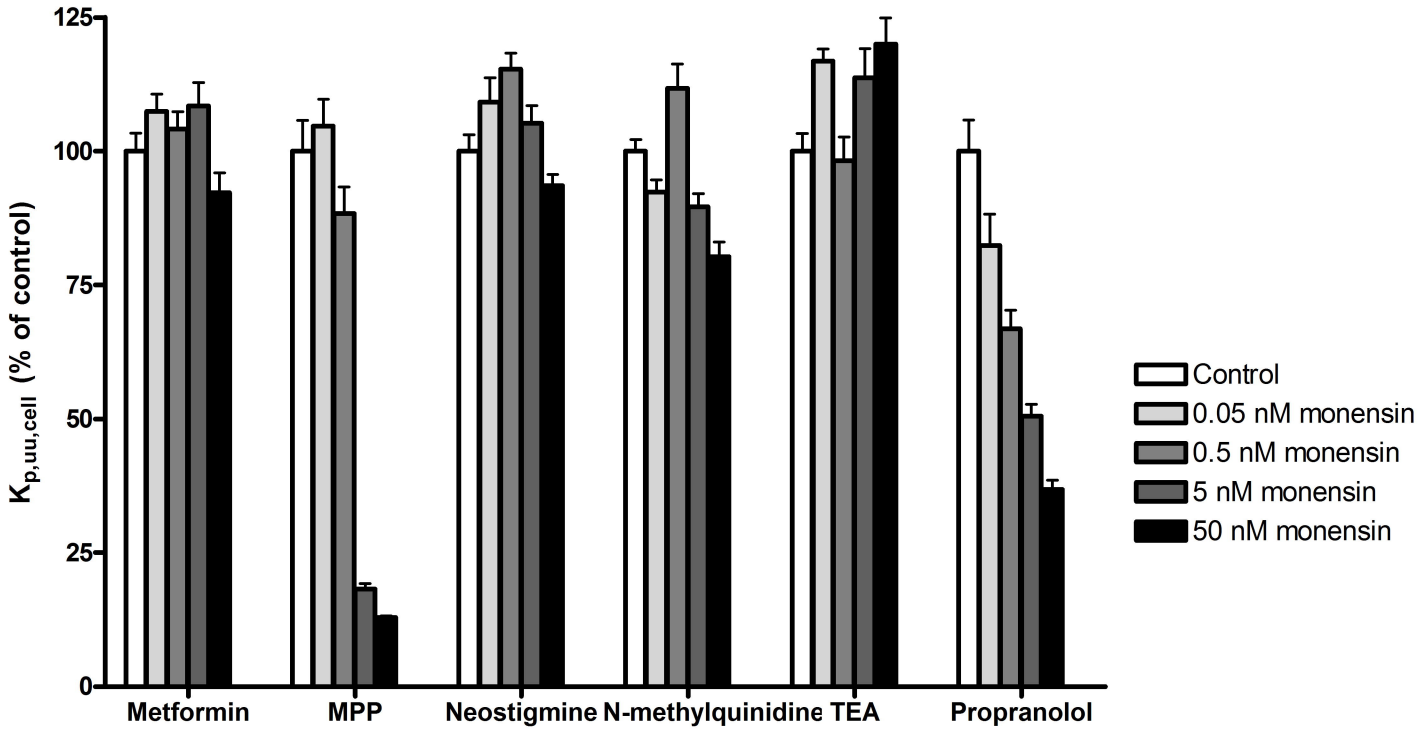
125
100
75
50
25
0
$K_{p,uu,cell}$ (% of control)
Metformin
MPP
Neostigmine
N-methylquinidine
TEA
Propranolol
Control
0.05 nM monensin
0.5 nM monensin
5 nM monensin
50 nM monensin

Fig 8

A

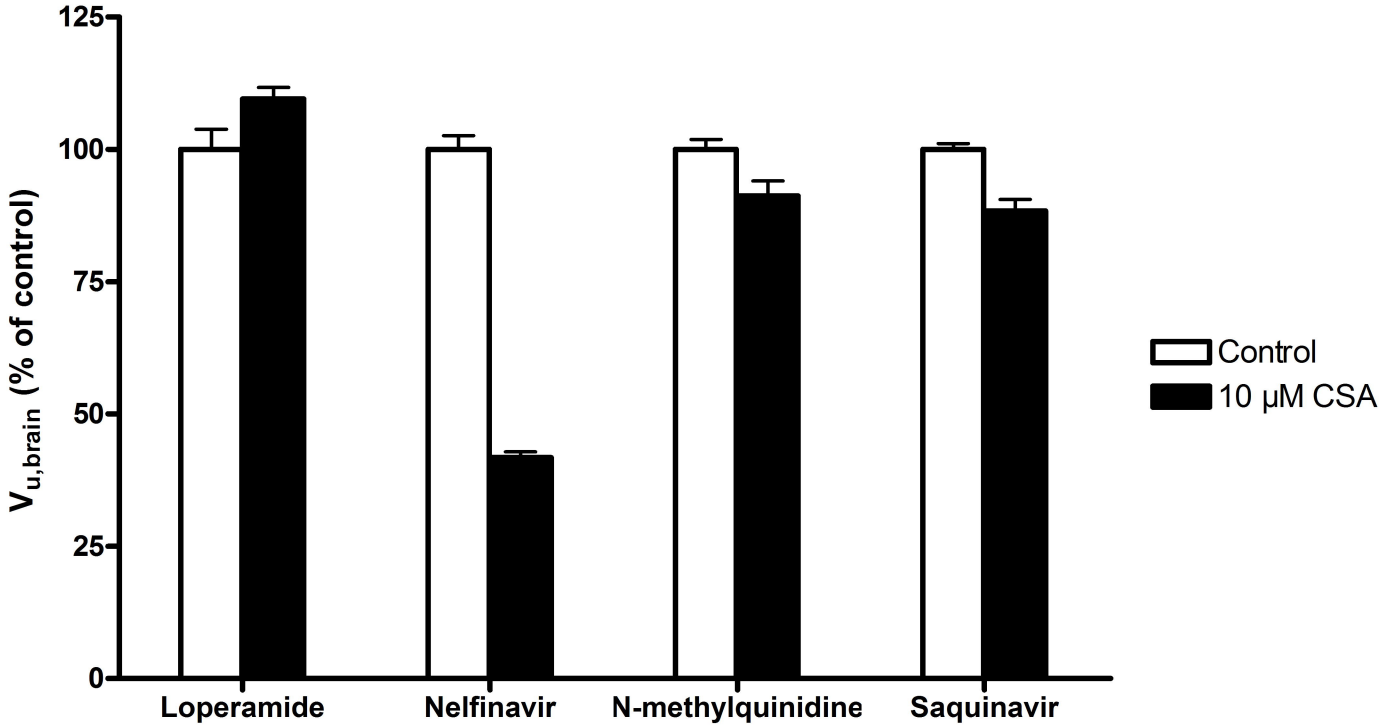
125
100
75
50
25
0
$V_{u,brain}$ (% of control)
Loperamide
Nelfinavir
N-methylquinidine
Saquinavir
Control
10 μM CSA

B

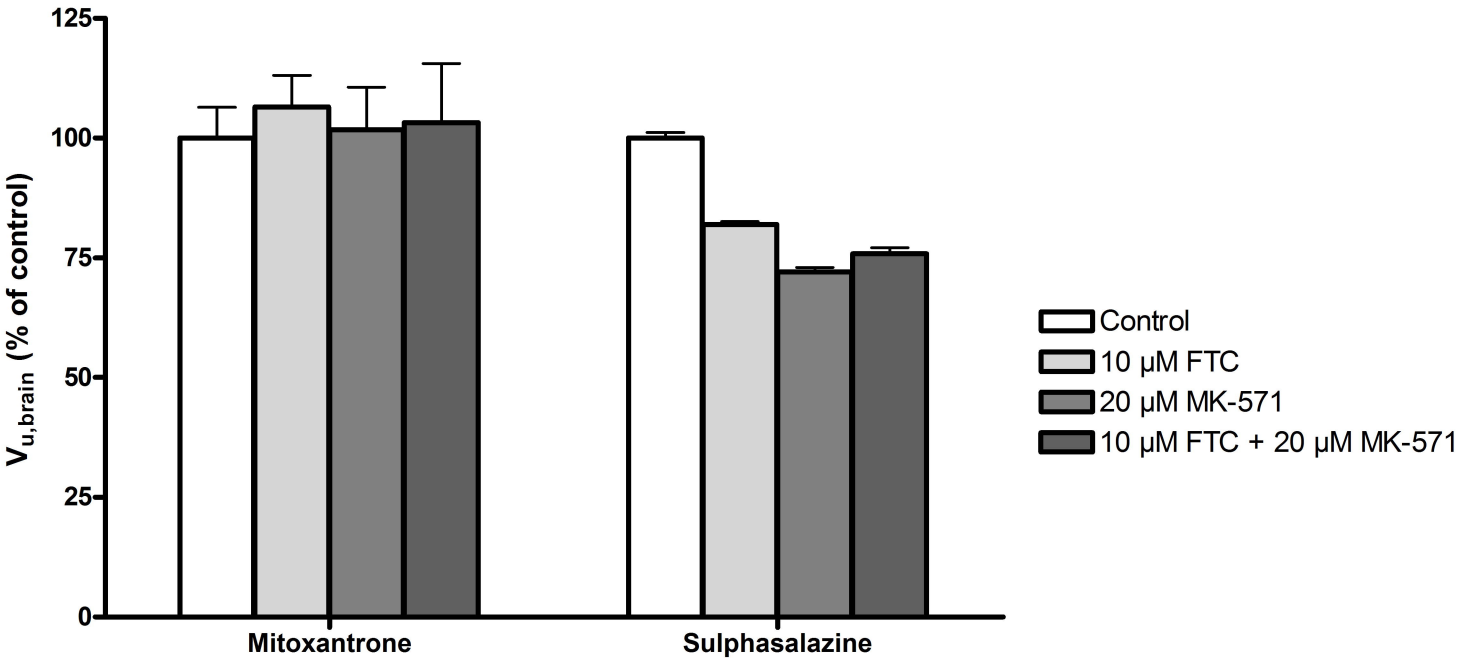
125
100
75
50
25
0
$V_{u,brain}$ (% of control)
Mitoxantrone
Sulphasalazine
Control
10 μM FTC
20 μM MK-571
10 μM FTC + 20 μM MK-571